



# An intensification of atmospheric CO<sub>2</sub> concentrations due to the surface temperature extremes in India

Smrati Gupta<sup>1,2</sup> · Yogesh K. Tiwari<sup>1,3</sup> · J. V. Revadekar<sup>1</sup> · Pramit Kumar Deb Burman<sup>1,3</sup> · Supriyo Chakraborty<sup>1,3</sup> · Palingamoorthy Gnanamoorthy<sup>4,5</sup>

Received: 17 April 2021 / Accepted: 6 September 2021 / Published online: 24 September 2021  
© The Author(s), under exclusive licence to Springer-Verlag GmbH Austria, part of Springer Nature 2021

## Abstract

The terrestrial biosphere plays a pivotal role in removing carbon from the atmosphere. The removal processes are primarily affected by the presence of extreme temperature in the atmosphere. Little information is available on carbon removal response by the terrestrial biosphere during extreme temperature events over the Indian region. India has witnessed frequent and intense heatwaves in the recent past, and future projections about the frequency of heatwave occurrence suggest a further increase in the changing climate scenario. This study used surface CO<sub>2</sub> flux observations and satellite retrieved columnar and mid-tropospheric CO<sub>2</sub> concentrations to understand atmospheric CO<sub>2</sub> variability and its transport patterns with anomalously high-temperature events such as heatwave conditions over India. Intensification of temperature up to 32 °C has increased the atmosphere-biosphere CO<sub>2</sub> fluxes (carbon sink). But further intensification in temperature (> 32–33 °C), like those observed during heatwaves, tends to drive the ecosystem to act as a CO<sub>2</sub> source into the atmosphere due to reduced ability to absorb atmospheric CO<sub>2</sub>. Such excess CO<sub>2</sub> fluxes may lead to change in the atmospheric CO<sub>2</sub> concentration via atmospheric circulation or the vertical transport of the air masses from the near-surface to the upper levels in the atmosphere. The satellite observed CO<sub>2</sub> concentration is elevated by 2–3 ppm during the heatwave conditions over India. The impact of extreme temperature on the biospheric sink capability in the carbon cycle, leading to an increase in the atmospheric CO<sub>2</sub> concentration, is one of the significant outcomes of this study.

## Abbreviations

GHG	Greenhouse gas
CO <sub>2</sub>	Carbon dioxide
XCO <sub>2</sub>	Columnar carbon dioxide
NEE	Net Ecosystem Exchange
PAR	Photosynthetically Active Radiation

NDVI	Normalized Difference Vegetation Index
ISMR	Indian Summer Monsoon Rainfall
MAM	March April May
AIRS	Atmospheric InfraRed Sounder
OCO-2	Orbiting Carbon Observatory-2
AMSL	Above Mean Sea Level
VPD	Vapour Pressure Deficit

Responsible Editor: Sang-Woo Kim.

✉ Yogesh K. Tiwari  
ykatiwari@tropmet.res.in

<sup>1</sup> Indian Institute of Tropical Meteorology, Ministry of Earth Sciences, Pune, India

<sup>2</sup> Institute of Environment and Sustainable Development, Banaras Hindu University, Varanasi, India

<sup>3</sup> Department of Atmospheric and Space Sciences, Savitribai Phule Pune University, Pune, India

<sup>4</sup> Coastal Systems Research, M. S. Swaminathan Research Foundation, Chennai, India

<sup>5</sup> Key Laboratory of Tropical Forest Ecology, Xishuangbanna Tropical Botanical Garden, Chinese Academy of Sciences, Menglun 666303, China

## 1 Introduction

During the last hundred years, the global mean surface temperatures have risen by 0.78 °C (IPCC 2013). Using observed data, Oza and Kishtawal (2015) have shown that India has a dominant tendency towards the warming period. Annual minimum temperature over more than 50% of India showed warming at the rate of 0.24 °C per decade (Rao et al. 2014). In most surface temperature data sets, the years 2014, 2015, and 2016 set new global heat records since regular in situ measurements started (Rahmstorf et al. 2017). For India, the annual average land surface air temperature

indicates 2016 as the warmest year since national records commenced in 1901 (Srivastava et al. 2017).

The pre-monsoon season in India, including March, April, and May (MAM), is a hot weather season, with the majority of heat waves occurring in May and sometimes in April. Almost the entire South Asian region experiences hot weather extremes in this season. Such recurring extremities have resulted in a severe societal loss. The frequency of hot days and hot nights showed a widespread, increasing trend. There was an increase in the number of hot days over the country during the pre-monsoon season, as reported by Kothawale et al. (2010). Similar features until the year 2015 were reported by Rohini et al. (2016). They suggested abnormal, persistent high atmospheric pressure at the surface with the anti-cyclonic flow supplemented with clear skies and depleted soil moisture is primarily responsible for the occurrence of the heatwaves over India. For the Indian region, Kothawale and Kumar (2005) reported a significant increasing trend of around 0.2 °C per decade in the annual mean, maximum, and minimum temperatures during the recent three decades of 1971–2003. Seasonal warming trends over different regions and temperature extremes of different intensities and duration have also been reported (Ray and De 2003; Roy and Balling 2005; Dash and Hunt 2007; Dash and Mamgain 2011). The recent year of 2015 was the third-warmest year since records commenced in 1901 based on the annual mean land surface air temperature averaged over India, which was 0.7 °C above the 1961–90 average (Srivastava et al. 2016). The increasing temperature trend over India is noticed for the last few decades; details can be found in Sanjay et al. (2020). A recent study by Perkins-Kirkpatrick and Lewis (2020) features the frequency of heatwaves increasing worldwide in the changing climate scenario, leading to more heat and warming. The vulnerability of the population rises with any change in the frequency or intensity of the heat waves. Many regions of the world, previously not affected by the heatwaves, are now reporting the loss of lives and economic losses due to intense heatwaves. In such an increased warming scenario of temperature trends and heatwave days, it becomes crucial to understand the biosphere's response in the presence of extremely high temperatures. This might affect the carbon sequestration capacity of the biospheric sink processes, which are a vital component in absorbing the global anthropogenic and natural CO<sub>2</sub> emissions.

Atmospheric CO<sub>2</sub> concentrations have broken all the records and reported the highest ever concentrations crossing 400 ppm in 2015 in recent times. India is one of the largest and fastest-growing economies in South Asia and experiencing high energy demand for its economic growth. Atmospheric CO<sub>2</sub> emissions in India are directly linked to economic growth (Udemba et al. 2020, 2021; Adebayo et al. 2021). Climate variabilities also modulate year-to-year

variation of atmospheric CO<sub>2</sub> concentrations. These variabilities are often studied in association with various large-scale phenomena such as El Nino, where warm conditions (higher sea surface temperatures than normal) showed increased atmospheric CO<sub>2</sub> concentrations (Kim et al. 2016; Kumar et al. 2016). Further, inter-annual variability associated with drought years of Indian Summer Monsoon Rainfall (ISMR) shows an increase in atmospheric CO<sub>2</sub> concentrations due to the decrease in NDVI and enhanced surface temperatures (Tiwari et al. 2014). Revadekar et al. (2016) studied the variation of atmospheric CO<sub>2</sub> concentrations during active/break phases (Inter-annual variability) of ISMR and showed that the break phases decrease the CO<sub>2</sub> concentrations in the atmosphere. This reduced concentration is mainly due to weak circulation in the atmosphere, and also, a stronger biospheric sink prevails during the break period (Valsala et al. 2013). Opposite features are seen during the active phase of the monsoon. Other than these, temperature variability has also been studied in link with the atmospheric CO<sub>2</sub> concentration levels, suggesting that these two vary together (Lüthi et al. 2008; Kumar et al. 2014). The year 2015 was a deficient summer monsoon rainfall season for India. In addition, it was a year when during the pre-monsoon months of MAM, intense heatwave occurrence led to the loss of more than 2500 human lives (Guha-Sapir et al. 2016; Rohini et al. 2016; Pattanaik et al. 2017). Previous studies, as mentioned, discussed the factors associated with the intensification of atmospheric CO<sub>2</sub> during a deficient summer rainfall season. The intensification related to extreme temperature events such as heatwave occurrence during the pre-monsoon season is to be explored.

Atmospheric CO<sub>2</sub> concentrations peak over the major parts of the Indian region during the MAM season; this is possibly due to reduced photosynthetic activity (weak biospheric sink) and elevated surface temperatures. Most of these studies are limited to annual to seasonal scales. One of the sub-seasonal modes of temperature variation characterized by anomalously high temperatures is observed as heatwaves, which may also alter the concentration of CO<sub>2</sub> in the atmosphere. The average summer temperature during MAM over India's northern plains goes beyond 30 °C and is aided by the prevailing heatwaves over this region. The temperature pattern during the heatwave period of 2015 is shown in Fig. 1a (detailed features are discussed in Sect. 3.1). Extreme high-temperature episodes are sometimes observed even during the onset of the summer monsoon rainfall season (June, July) at several stations over India. CO<sub>2</sub> loading in the atmosphere is suspected to be due to the higher temperatures and weak photosynthetic activity. Therefore, it becomes vital to understand the variability of CO<sub>2</sub> in the presence of extreme temperature episodes over India. As surface CO<sub>2</sub> observations are sparse in India, it becomes difficult to study this problem on a country scale. To investigate

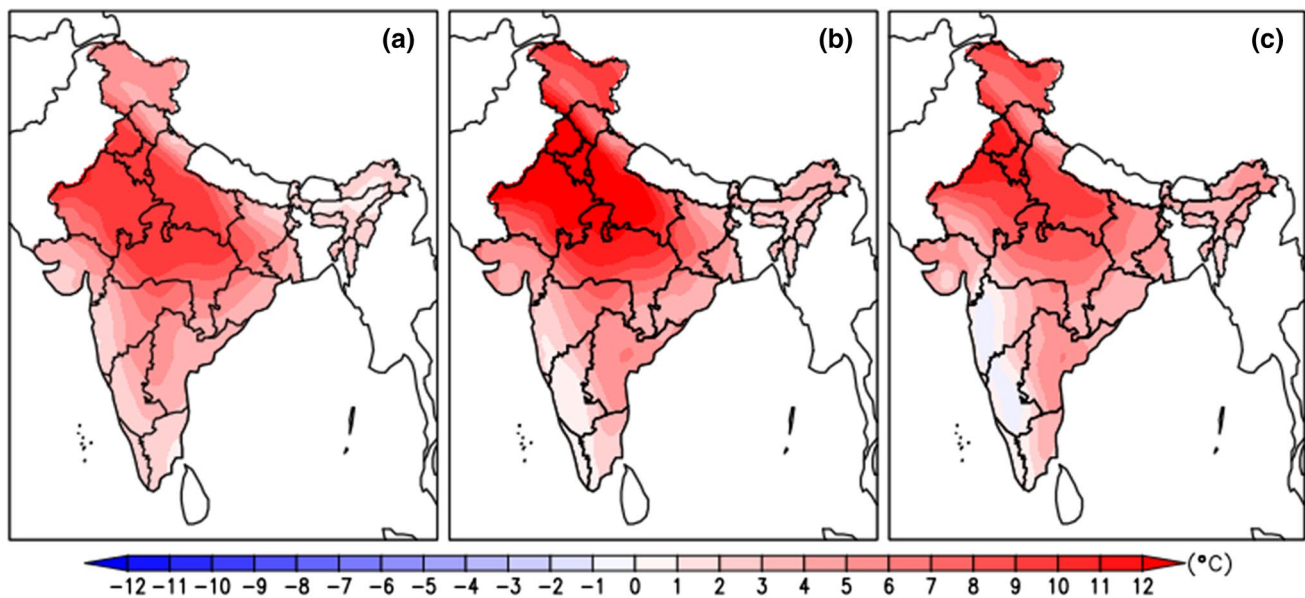


**Fig. 1** Spatial distribution of detrended surface temperature during **a** prolonged heatwave of the year 2015, **b** difference between temperatures during the heatwave and non-heatwave period of the year 2015,

and **c** difference between temperatures during the heatwave and non-heatwave period for the mean period 2004–2015

this, we utilized eddy-covariance-based surface CO<sub>2</sub> flux observations, satellites OCO-2 and AIRS retrievals, and Era-interim meteorological parameters (e.g., surface temperature and winds) during heatwave conditions in India. Anomalous features in satellite retrieved CO<sub>2</sub> concentration, and wind circulation patterns, are examined in this study, studying the case of intense heatwave occurrence during 2015. Circulation parameters may have been responsible for changes in observed CO<sub>2</sub> distribution in the troposphere. This study is the first attempt to report the intensification of CO<sub>2</sub> emissions hence the atmospheric concentrations, linked to the extreme high-temperature occurrences such as heatwaves over the Indian region.

## 2 Data and methodology

### 2.1 Surface CO<sub>2</sub> flux observations

We use the surface CO<sub>2</sub> fluxes called Net Ecosystem Exchange (NEE) from two different ecosystems over India. These are from an agricultural ecosystem, Barkachha in north India (Deb Burman et al. 2020), and Pichavaram mangrove forest in south India (Gnanamoorthy et al. 2020). Surface CO<sub>2</sub> flux (NEE) observations shown in Fig. 2 are from the BarkachhaBarkacha site, obtained during 2014–2016, phase III of Cloud-Aerosol Interaction and Precipitation Enhancement Experiment (CAIPEEX) (Prabha et al. 2011). As part of the ground campaign, a 20 m tall tower was erected in the south campus of the Banaras Hindu University

at Barkachha (25.06° N, 82.59° E, 169 m AMSL), approximately 90 km southwest of the Varanasi city in the state of Uttar Pradesh, India (Resmi et al. 2019; Sathyanadh et al. 2017). An eddy covariance (EC) setup was installed on the tower at 5 m height, consisting of a WindMaster Pro 3D sonic anemometer-thermometer (Gill Instruments, Lymington, UK) and an open-path infrared CO<sub>2</sub>–H<sub>2</sub>O analyzer (IRGA) LI7500A (Li-COR Inc. Lincoln, Nebraska, USA). The half-hourly CO<sub>2</sub> flux (NEE in  $\mu\text{mol m}^{-2} \text{s}^{-1}$ ) has been calculated using these 10 Hz EC measurements by the Reynolds averaging method (Aubinet et al. 1999). A set of recommended pre- and post-flux calculation quality control measures, including linear detrending, have been applied to remove various noises and ensure the quality and acceptability of the flux data. The details about the flux calculation and quality control measures can be found in Deb Burman et al. (2020). The half-hourly air temperature ( $T_{\text{air}}$  in °C) was measured by a WXT520 (Vaisala Oyj, Vantaa, Finland) multi-component weather sensor at 3 m on the tower and saved in a CR3000 data-logger (Campbell Scientific, Logan, Utah, USA).

The data used in Fig. 3 is from the Pichavaram tropical mangrove wetland (lat. 11° 20' N; long. 79° 55' E, the location is shown in Fig. 2d). This site is a part of a micro-meteorological observational network based on the Eddy Covariance (EC) technique, named MetFlux India, operated by IITM Pune and funded by the Ministry of Earth Sciences, the Government of India (Chakraborty et al. 2020). NEE observations during the MAM months of the year 2018 are plotted against the ambient air temperature ( $T_{\text{air}}$ ) in Fig. 3a.

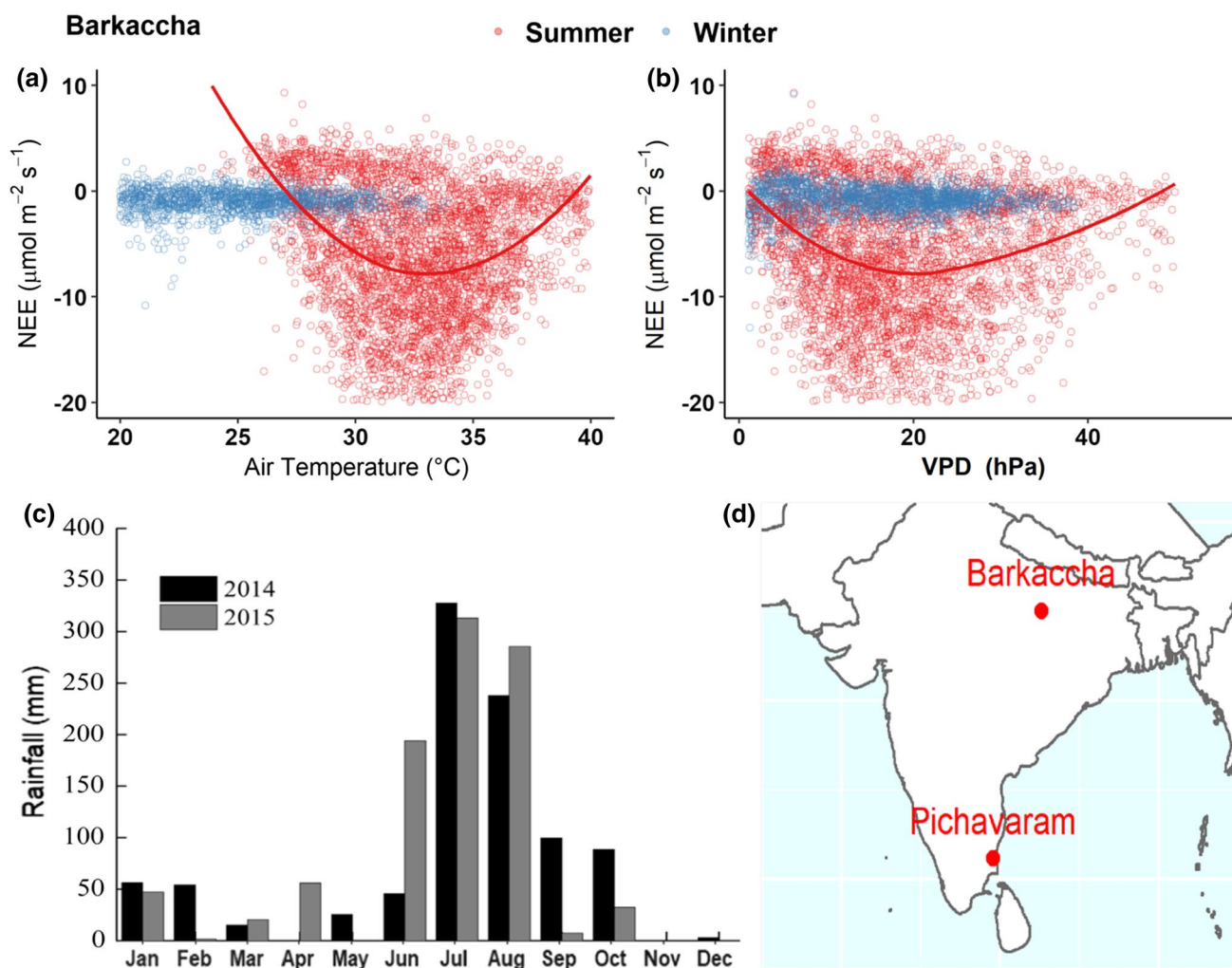


**Fig. 2** The dependence NEE on **a** air temperature and **b** vapor pressure deficit (VPD) during summer monsoon months of 2014–2016 at Barkaccha, Uttar Pradesh, India. Red circles (blue circles) show sum-

mer monsoon months during JJAS (winter months during DJF). The solid lines (red) are regression lines, **c** cumulative monthly rainfall at Barkaccha, and **d** location of observation sites (red circles)

The details about the flux calculation and quality control measures are available in Gnanamoorthy et al. (2020). The half-hourly air temperature ( $T_{\text{air}}$  in  $^{\circ}\text{C}$ ) was measured by a WXT520 (Vaisala Oyj, Vantaa, Finland) multi-component weather sensor at 2 m, 6 m, and 10 m on the tower and saved in a CR3000 data-logger (Campbell Scientific, Logan, Utah, USA). In Figs. 2 and 3, only the daytime measurements are considered.

## 2.2 Satellite measured $\text{CO}_2$ concentration

This study used  $\text{CO}_2$  concentrations retrieved from Orbiting Carbon Observatory-2 (OCO-2) and Atmospheric Infrared Sounder (AIRS) aboard Aqua satellite over the Indian domain. AIRS has been functional since 2002 and OCO-2 since September 2014.  $\text{CO}_2$  retrievals from these satellites have been used in many studies and proved reliable in

revealing the  $\text{CO}_2$  distribution globally and regionally in the troposphere (Jiang et al. 2010; Kumar et al. 2016; Revadekar et al. 2016; Golkar et al. 2020). The short wave infra-red (SWIR) band enables OCO-2 to capture the variation in  $\text{XCO}_2$  due to the fluctuation in source and sinks. OCO-2 instrument covers  $1.29 \text{ km} \times 2.25 \text{ km}$  footprint at nadir, and acquiring up to eight such footprints provides overall swath width of 10.3 km. It measures the  $\text{XCO}_2$  combining the measurements in its three spectral bands with a standard deviation within 1.5 ppm (Wu et al. 2018).  $\text{XCO}_2$  data of OCO-2 downloaded in a gridded format from NASA's website <https://co2.jpl.nasa.gov/> at  $100 \text{ km} \times 100 \text{ km}$  grid spacing and averaged to  $250 \text{ km} \times 250 \text{ km}$  to match it with the resolution of AIRS retrievals. With its high resolution and SWIR sensors, OCO-2 can better capture the variations near the earth's surface in sources and sink. This data is available from September 2014 onwards, which is insufficient



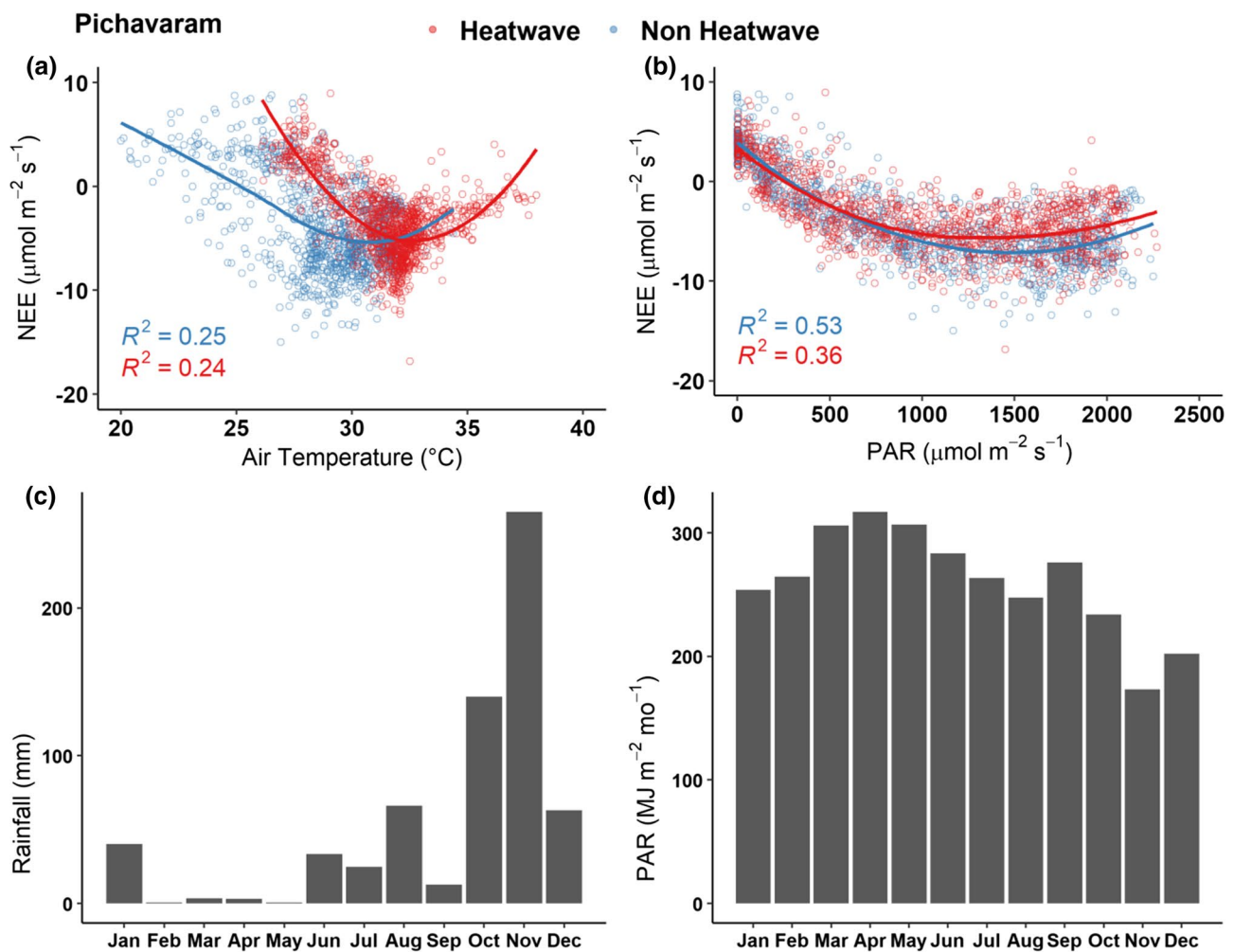


**Fig. 3** The dependence of NEE on **a** air temperature and **b** photosynthetically active radiation (PAR) in the daytimes of MAM months during 2018. **c** monthly total rainfall (in mm) and **d** monthly total PAR recorded in the study area for a 1-year duration between October 2017 to September 2018. Here the data plotted in red is for the

heatwave and blue for the non-heatwave period with their respective regression lines. (number of data points ‘*n*’ for calculating regression are 1154 for the heatwave, 1117 for non-heatwave, and the  $R^2$  values indicated here are with  $p$ -values  $< 0.05$ ) plotted over the NEE observations

to understand any long-term mean and inferences. With its wider swath at nadir ( $90 \text{ km} \times 90 \text{ km}$ ), AIRS can cover the globe in a single day. Retrievals from observed radiance are performed using a vanishing partial derivative algorithm. The high spectral resolution of the AIRS instrument provides CO<sub>2</sub> monitoring accuracy up to 1–2 ppm. The presence of the AMSU unit aids in retrieving cloud-free data over the globe. To understand the long-term variation in this study, we have used AIRS level 3, version 5, a gridded data from 2004 to 2015 (12 years). More details about the satellite, data products, and retrieval algorithms about AIRS are available in Chahine et al. (2005, 2008); Olsen and Licata (2015). Both XCO<sub>2</sub> and CO<sub>2</sub> retrievals were detrended to discard the effect due to the global increase in atmospheric CO<sub>2</sub>. Since the heatwave conditions over India are short-period events, the number of observed satellite pixels during these

conditions is insufficient for studying the variation on the same time scale. Therefore, we have used satellite data from 15 April to 30 May, covering most heatwave conditions over India (denoted as heatwave period hereafter).

### 2.3 Atmospheric circulations parameters and surface temperature data

Meteorological variables used in this study are from Era-interim data products. Era-interim data from the European Centre for Medium-Range Weather Forecasts (ECMWF) was generated using a four-dimensional variational analysis assimilation method. It is available in the high spatial and temporal resolution of 79 km (T255 spectral resolution), four times daily, and 60 levels in vertical up to 0.1 hPa in gridded format. Observation data obtained worldwide given as

inputs to the model are quality checked, controlled, and then an assimilation scheme is applied to generate the reanalysis products. The data selected for our study is from 2004 to 2015. Parameters used here are daily data of zonal, meridional, vertical wind components, and surface temperature. This data has been extensively used in atmospheric research studies to understand the atmospheric state in several studies. Rainfall data used at Barkachha observational site is from India Meteorological Department (IMD).

### 3 Results and discussion

#### 3.1 Intensification of surface temperature

Surface temperature intensifies over India, mainly during the summer months (MAM). Higher temperature conditions are referred to as heatwaves. Globally there is no standard definition adapted to define the heatwaves. Different regions may classify the criteria to determine the extent of heatwave depending upon a threshold conducive to the respective geographical and climatic conditions. However, the heatwave is higher than the average maximum temperature in the region, which leads to discomfort in the population's general well-being. During the pre-monsoon season, spells of hot weather occasionally occur over certain parts of India. India's weather was significantly warmer than usual during 2015, in line with the warmer than average global climate observed. The annual mean land surface air temperature averaged over the country during 2015 was  $+0.67\text{ }^{\circ}\text{C}$  above 1961–1990. As per IMD, 2015 was the third-warmest year in India since 1901, and it had witnessed intense heatwave (Srivastava et al. 2016; Pattanaik et al. 2017). States such as Andhra Pradesh, Odisha, Gujarat, Madhya Pradesh, Vidarbha region of Maharashtra, etc., witnessed this intense heatwave in 2015. 2015 heatwave was especially prevalent over the Andhra Pradesh and Telangana during the pre-monsoon season from 15 April to 30 May. More minor heatwave episodes of 1–5 days were seen over various regions of central India. As reported in the seasonal weather report of IMD (Mausam 2016), severe and widespread heatwave conditions were observed over most parts of north/north-western, central, eastern, and southeast peninsular India during the second fortnight of May month.

The annual cycle of mean surface air temperature over India shows a continuous increase from January to May. Pre-monsoon months (MAM) witnesses high surface temperature. As per India's climate diagnostics bulletin April and May, 2015 (<http://rcc.imdpune.gov.in/Products.html>) severe and widespread heatwave conditions occurred over most parts of north/north-western, central and eastern India from 15 April to 30 May 2015. However, the rest of the country experienced below-average temperature concerning the

long-term mean. Figure 1a shows surface temperature variations using Era-interim high-resolution detrended temperature data during the heatwave period of 2015. Most heatwave conditions prevailed during April and May, and a temperature rise was observed during this period. The surge was seen highest over the northwest region and extends towards the southeast region, covering central India. Figure 1b shows the temperature difference during the heatwave and non-heatwave periods of the MAM season of the year 2015. The pattern of maximum increase in temperature extends from the northwest region towards southeast India. Figure 1c shows the temperature difference between the heatwave and the non-heatwave periods of the MAM seasons for the mean period of 2004–2015. The usual increase was observed during 2004–2015 (mean) (Fig. 1c). However, the extent of warming and spatial distribution of temperature was greater than usual for a year when a pronounced heatwave occurred, such as in 2015 (Fig. 1b).

#### 3.2 Observed surface CO<sub>2</sub> fluxes

Figure 2 shows the NEE observed during CAIPEEX-IGOC (Prabha et al. 2011) measurement campaign during 2014–2016 at Barkachha, Uttar Pradesh, located in India's northern plains. The average summer temperature during MAM over the northern plains goes beyond  $30\text{ }^{\circ}\text{C}$  with a maximum of  $38\text{ }^{\circ}\text{C}$  during prevailing heatwave conditions (Barkachha station data, [www.imd.gov.in](http://www.imd.gov.in)). NEE tends to increase at  $35\text{ }^{\circ}\text{C}$  temperature during the summer and remains almost constant during winter (Fig. 2a). While during summer, where the average temperature of this area goes beyond  $30\text{ }^{\circ}\text{C}$ , NEE tends to negative (decreasing) values, signifying more exchange between flora and environment, resulting in increased carbon fixation by the biosphere. Hence, the ecosystem acts as a sink of atmospheric CO<sub>2</sub>. However, NEE further increases at higher temperatures (more than  $35\text{ }^{\circ}\text{C}$ ). Figure 2b shows NEE variation with Vapour Pressure Deficit (VPD) values during the summer and winter months. In a similar pattern, NEE decreases till 20 hPa VPD and increases beyond. Such tendency suggests the sequestration capacity was reduced due to the prevailing high VPD. The sunlight is abundantly available during the summer season, so is the rainfall during JJAS (Fig. 2c) may not be a limiting factor for this ecosystem. Thus for this site, it can be said from Fig. 2a that this tendency to go towards positive NEE may be driven by the prevailing higher temperature and reduced soil moisture (large VPD) even when the rainfall activity is significant. Previous studies have suggested that during the summer monsoon season, while the rainfall is abundant, VPD remains significantly high near the surface (Ramaraio et al. 2019). When the flora is stressed, its

capacity of fixing the atmospheric CO<sub>2</sub> under high temperatures is reduced due to stomatal closure.

Consequently, the atmospheric CO<sub>2</sub>, instead of getting fixed by flora, tends to remain in the atmosphere, leading to higher than the average atmospheric CO<sub>2</sub> concentrations near the biosphere. Thus, the above analysis shows that the biospheric sink capacity is severely affected in the presence of high temperatures. Such high temperatures are also observed during a heatwave period. To study the biospheric response to the heatwave, data from Barkaccha is not available during MAM months when most of the heatwave occurs. Data from another site Pichavaram were utilized further in this study.

The data shown in Fig. 3 is from the Pichavaram site of the MetFlux India Project for the MAM months of 2018. During this season, a transition from the post-monsoon or winter season (of this region) to summer occurs, and the average temperature of this area goes beyond 30 °C. Figure 3a shows the variation of NEE with the temperature during the heatwave and non-heatwave periods. During MAM, NEE values become more negative with the increase in temperature, signifying more exchange between flora and the environment, resulting in more CO<sub>2</sub> fixed by the biosphere; hence, the ecosystem acts as a sink to the atmospheric CO<sub>2</sub>. However, at temperatures around 32–33 °C, NEE stabilizes and tends towards positive at further higher temperatures (more than 36 °C). It is to be noted that MAM is a period of availability of the least amount of rainfall and the highest amount of photosynthetically active radiation (PAR) in this region (Fig. 3c, d). PAR is a part of the solar electromagnetic radiation spectrum in the range of 400–700 nm and is used as a source of energy for the photosynthesis of green plants. As PAR's availability is abundant during these MAM months, NEE tends to decrease initially, indicating active photosynthesis by the biosphere resulting in more atmospheric CO<sub>2</sub> fixation (Fig. 3b). However, the tendency towards positive values of NEE was seen for the higher amount of PAR. The correlation between NEE and PAR also reduces ( $R^2$  changes from 0.53 to 0.36,  $p < 0.05$ ) during the heatwave condition, indicating the role of limiting factors for photosynthesis, even in the presence of high PAR. This tendency towards positive NEE values may be due to prevailing higher temperatures but the reduced soil moisture due to a lack of rainfall during these periods at this location during the MAM months. The biosphere stress results in a weak sink of CO<sub>2</sub> under high temperatures, mainly due to stomatal closure. Consequently, the atmospheric CO<sub>2</sub>, instead of getting fixed by flora, tends to remain in the atmosphere leading to higher than the average atmospheric CO<sub>2</sub> concentrations near the surface. Our finding is similar to the work done by Geddes et al. (2014) (over Canadian mixed forest) and Wohlfahrt et al. (2018) (for

Mediterranean forest ecosystems), who report carbon uptake by natural ecosystems to be severely affected by the heatwaves.

These observations from two different sites demonstrate the biosphere's behavior in the presence of extreme temperature limited by various climatic factors. Rainfall is the limiting factor for the Pichavaram site in the pre-monsoon months and VPD being the limiting factor for the Barkaccha site. It depicts that, in the presence of extremely high temperatures, the carbon uptake by the biosphere is severely compromised in an ecosystem. The magnitude of biosphere response to carbon sequestration process in the presence of extreme temperature may vary according to the type of biospheric constituents, such as the type of biomes, climatic conditions, and intensity and duration of prevailing temperatures. However, the biosphere response towards extremely high temperatures can be understood with the help of this analysis. This study suggests that high-temperature events such as those observed during heatwaves and the summer season reduce carbon sink by the biosphere.

### 3.3 Distribution of CO<sub>2</sub> concentration in the atmosphere

Considering the relation between temperature and surface fluxes of CO<sub>2</sub> that we perceive from Figs. 2 and 3 and also in the studies discussed above, an attempt is made in this section to study the variation in atmospheric CO<sub>2</sub> concentrations, i.e., XCO<sub>2</sub> from the OCO-2 satellite and free troposphere CO<sub>2</sub> concentrations from the AIRS satellite during the heatwave period of 2015. The distribution of detrended XCO<sub>2</sub> (OCO-2) and detrended free troposphere CO<sub>2</sub> concentration (AIRS) over the Indian region during the heatwave period of the year 2015 is shown in Fig. 4a and c, respectively. Both XCO<sub>2</sub> and CO<sub>2</sub> concentrations were high (positive values in the red shade) during the heatwave period over a major part of the Indian region. CO<sub>2</sub> concentrations during the heatwave period are compared with the non-heatwave period of the same MAM season of the year 2015 in Fig. 4b (of OCO2-XCO<sub>2</sub> concentrations) and Fig. 4d (of AIRS-CO<sub>2</sub> concentrations). Figure 4b shows the increase in XCO<sub>2</sub> concentration by 2–3 ppm or more, and Fig. 4d also indicates an increase in free troposphere CO<sub>2</sub> (even up to 8 ppm over certain regions) during the 2015 heatwave period in comparison to the non-heatwave period of the same year over a significant part of India. Both Fig. 4b and d showed an increase in CO<sub>2</sub> concentrations within a season, suggesting a contribution of the sub-seasonal variation to such observed increased concentrations. The average difference in CO<sub>2</sub> concentrations between a heatwave and a non-heatwave period for the long-term period of 2004–2015 was also analyzed and found to be lower than the difference seen during 2015

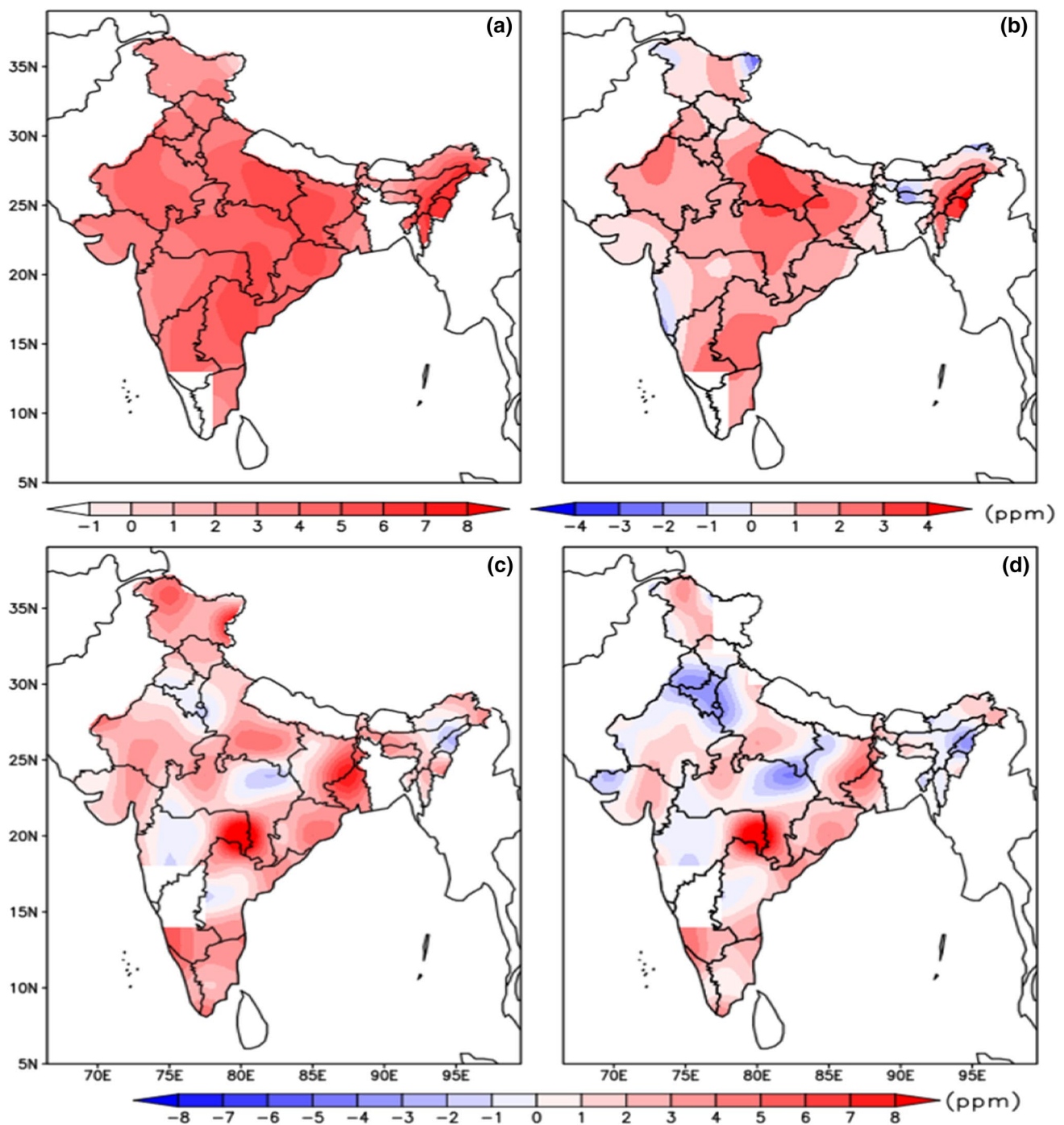


**Fig. 4** **a** Spatial distribution of detrended  $XCO_2$  (OCO-2) averaged during heatwave period of the year 2015, **b** difference in  $XCO_2$  between heatwave and non-heatwave period of 2015, **c** spatial distribution of detrended free troposphere  $CO_2$  concentration (AIRS) averaged during heatwave period of the year 2015, **d** difference in  $CO_2$  concentration between heatwave and non-heatwave period of 2015

Figure 4c, d also shows elevated  $CO_2$  over certain southern parts of India. Vidarbha, Telangana, and Andhra Pradesh regions reportedly observed longer spells of heatwave conditions during 2015, as mentioned in Sect. 3.1. As discussed in the previous section, this increase in  $XCO_2$  and  $CO_2$  concentration in the atmosphere could be related to

(figure not shown). This higher sub-seasonal increase in atmospheric  $CO_2$  concentration for a year with significant heatwaves (2015) was seen to be pronounced spatially and in magnitude (Fig. 4d). The increase in both  $XCO_2$  and atmospheric  $CO_2$  clearly shows that the enhancement of  $CO_2$  occurred during heatwave conditions over India.

Figure 4c, d also shows elevated  $CO_2$  over certain southern parts of India. Vidarbha, Telangana, and Andhra Pradesh regions reportedly observed longer spells of heatwave conditions during 2015, as mentioned in Sect. 3.1. As discussed in the previous section, this increase in  $XCO_2$  and  $CO_2$  concentration in the atmosphere could be related to



extra CO<sub>2</sub> concentration near the surface due to weaker absorption by the biosphere. The transport mechanism of the near-surface CO<sub>2</sub> to the upper levels in the troposphere is discussed next.

### 3.4 Atmospheric circulation patterns

Any fluctuation in the observed atmospheric CO<sub>2</sub> concentrations reflected up to the higher levels in the atmosphere results from the change in surface emissions acted upon by the active vertical transport processes. Kumar et al. (2014) have studied the CO<sub>2</sub> variability during different seasons and

its association with the climatic parameters over India from 2004 to 2011 to understand transport mechanisms. Further, Revadekar et al. (2016) have examined the intra-seasonal variability of CO<sub>2</sub> and suggested its association with anomalies in mid-tropospheric CO<sub>2</sub>. During the pre-monsoon season (MAM), the country experiences heatwave conditions and thus leads to more vigorous convection and transport of atmospheric constituents in the vertical direction. Therefore circulation patterns are examined during the heatwave period of the year 2015. Figure 5 shows the spatial distribution of zonal (u), meridional (v), and vertical components (w) of surface winds at 925 hPa during the heatwave period of the

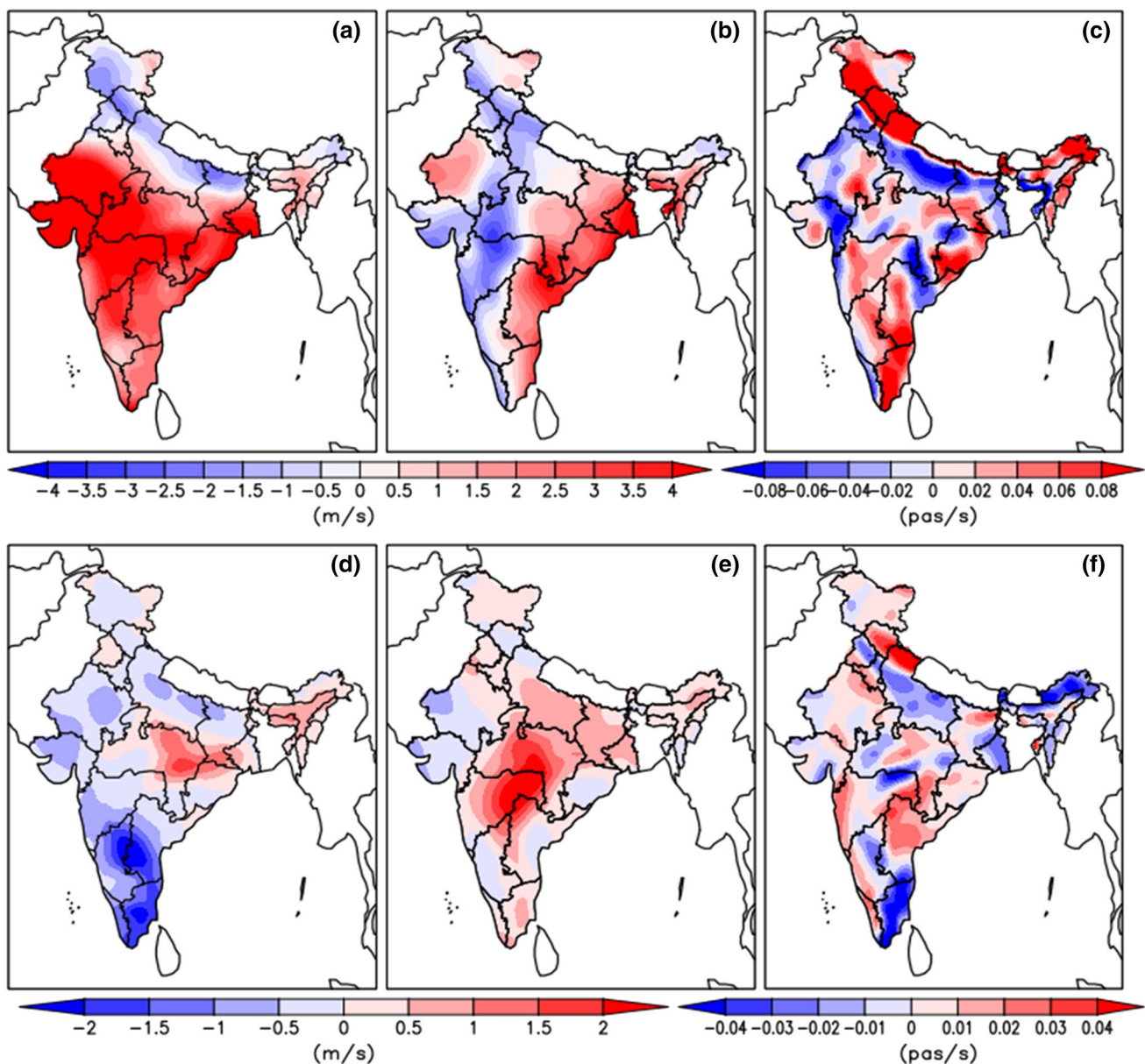


**Fig. 5** Spatial distribution of wind **a–c** all three components u,v,w during heatwave period of 2015, **d–f** difference between heatwave period of 2015 and 2004–2015 (mean)

year 2015 (Fig. 5, upper panel) and the difference of heatwave period of 2015 with the mean of the years 2004–2015 (Fig. 5, lower panel). The distribution of the zonal component of wind (Fig. 5d) shows positive anomalies over central parts of India and negative anomalies over the southernmost and northernmost parts of the country, indicating strong westerly over central parts and easterlies over the rest of the country. The distribution of the meridional component of wind (Fig. 5e) shows positive anomalies over the southern part of India, indicating a strengthening of southerlies over the region. Similarly, the vertical components (Fig. 5f) suggest strengthening vertical transport over a wide area of Indian landmasses. Thus, it indicates the strengthening of circulation pattern with strengthening of upward wind during the heatwave due to convection, supported by advection due to strengthening surface wind.

Spatial distribution of the difference in zonal, meridional and vertical components of surface winds during the heatwave period with the non-heatwave period (at 925 hPa) of the year 2015 is also examined in Fig. 6 (upper panel). The lower panel of Fig. 6 shows the difference in the heatwave

and non-heatwave periods in the mean period of 2004–2015. This pattern indicates the strengthening of westerlies over a large part of India and the enhancement of southerlies over the northeast region as convective activities being set over the northeast and central Indian region. Moreover, as shown in the upper panel, further enhancements in all three zonal, meridional, and vertical wind components indicate the more robust transport processes during heatwave conditions.

Thus, during the heatwave period, wind circulation patterns become more substantial concerning mean circulation during the long period of 2004–2015. It is also more robust than the non-heatwave period of the same season of MAM. Thus, the strengthening of circulation patterns associated with the heatwave, causing vertical transport of excess near-surface atmospheric  $\text{CO}_2$ , supports the increase in  $\text{CO}_2$  levels in the upper atmosphere as seen in Fig. 4a, c of the spatial distribution of  $\text{CO}_2$  over the Indian region.

An increase in  $\text{CO}_2$  concentration during the drought years of Indian summer monsoon months JJAS, primarily driven by higher surface temperature, was already reported in the Indian context by Tiwari et al. (2014). They

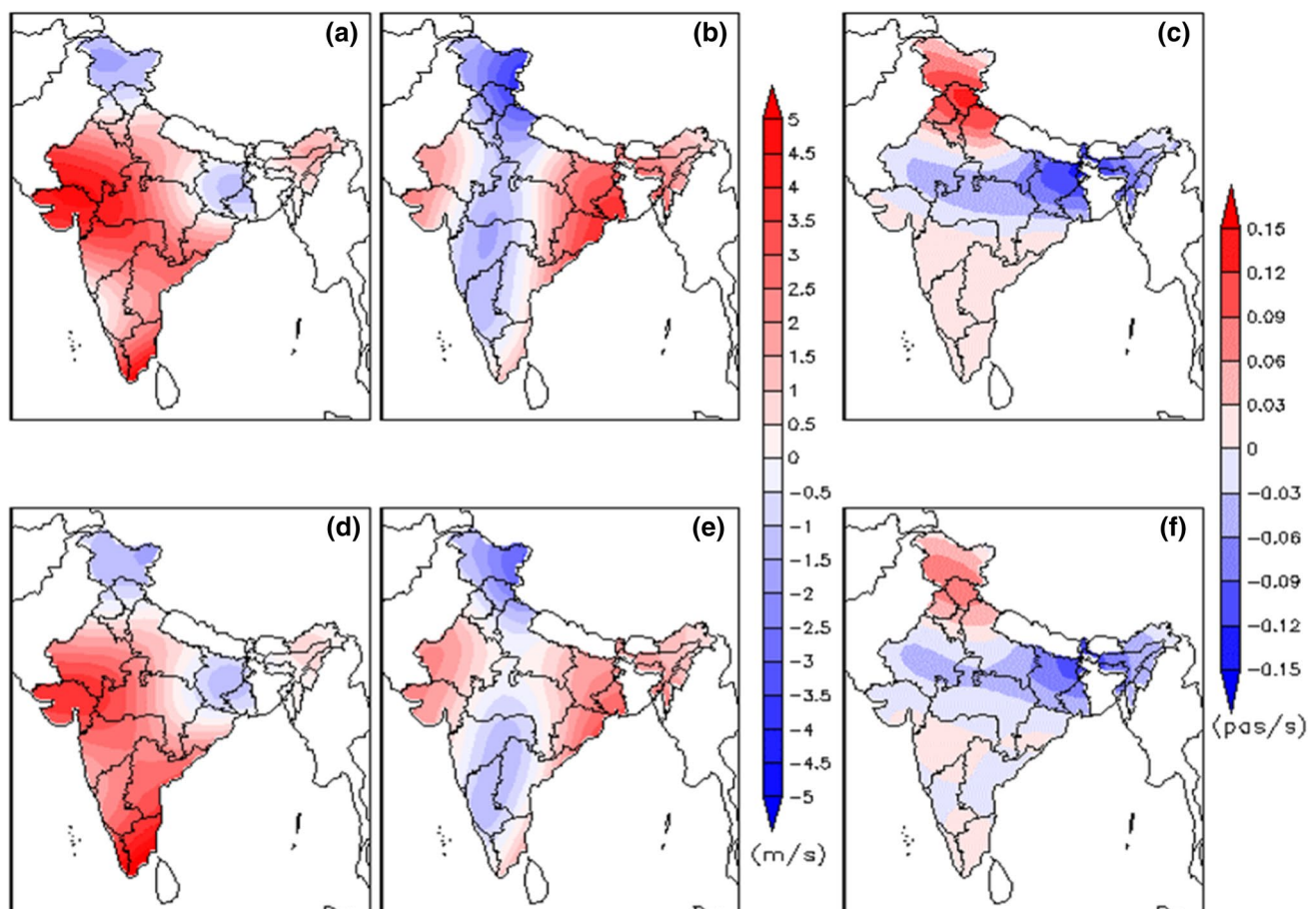


**Fig. 6** Spatial distribution of wind **a–c** all three components  $u, v, w$ ; difference during the heatwave and non-heatwave period of 2015, **d–f** difference between heatwave and non-heatwave period of 2004–2015 (mean)

suggested the weaker circulation during decreased rainfall season aided by reduced NDVI due to the reported increase in CO<sub>2</sub>. Though there is an increased temperature anomaly during drought years, it is in the range of 0.2–0.6 °C, while heatwaves are extreme temperature events with temperature anomalies at least 4–5 °C in general. In addition, the circulation parameters associated with such high temperatures are found to be different. It is observed that circulation is strengthened during the heatwave period, while the drought years are associated with weaker atmospheric circulation patterns.

## 4 Conclusions

The seasonality observed in CO<sub>2</sub> concentrations in India peaks during MAM months. These months observe intense heatwaves in India. The biosphere, being a carbon pool, removes a substantial amount of CO<sub>2</sub> from the atmosphere. Still, the removal process is affected mainly by the occurrence of high temperatures events in the atmosphere.

The biosphere is a significant sink of atmospheric CO<sub>2</sub>; however, we see that the variabilities associated with atmospheric processes affect the sinking capacity of the biosphere. Previous studies reported monsoon droughts as one of the reasons for decreased biospheric sink capacity. There is not much information about CO<sub>2</sub> variability during heatwave conditions in India due to the limited coverage and frequency of observation in the Indian region. In the present study, we explored the mechanism behind heatwaves and extreme temperature episodes being other causes of the decrease in the biospheric sink. We elaborated with the help of observations that a reduction in the biospheric sink, acted upon by prevailing anomalous atmospheric circulation occurring during the heatwaves, may lead to the observed increase in atmospheric CO<sub>2</sub> concentrations. In this study, we used eddy-covariance-based surface CO<sub>2</sub> flux (NEE) observations, satellite observations, and meteorological parameters to examine columnar CO<sub>2</sub> and atmospheric CO<sub>2</sub> variability during anomalous temperature rise in India. Our study reveals:

- NEE in a forest ecosystem was reduced during heatwave conditions, leaving excess CO<sub>2</sub> in the atmosphere. In addition, NEE in an agricultural ecosystem was reduced owing to very high temperatures.
- Strengthening of circulation parameters associated with the heatwave supports the increase in CO<sub>2</sub> levels in the upper atmosphere
- Satellite observed CO<sub>2</sub> concentrations during the heatwave conditions are elevated by 2–3 ppm compared to the non-heatwave period.

The satellite observed CO<sub>2</sub> concentration elevated during heatwave conditions over the Indian region. These are mainly due to high surface temperature, weak terrestrial biospheric CO<sub>2</sub> sink, and strong vertical air mass transport over the Indian region. With the projected increase in the frequency of heatwaves worldwide, this might enhance atmospheric CO<sub>2</sub> concentrations globally, leading to a further rise in projected atmospheric CO<sub>2</sub> values observed at monitoring stations. This study signifies the importance of combining heatwave impacts in the biospheric component of global carbon cycle studies. To quantify these findings, surface observations network and continuous satellite data with the high-resolution biospheric model are prerequisites. The quantification of CO<sub>2</sub> emissions during heatwave conditions will help us understand the CO<sub>2</sub> intra-seasonal variations in India. In addition, it will be an essential factor in understanding CO<sub>2</sub> emission estimates using a top-down modeling approach. This study advocates an accurate and robust surface CO<sub>2</sub> monitoring network with a high-resolution modeling framework in India.

**Acknowledgements** We thank the Director, IITM, Pune, and MoES, GOI, for facilitating this research work. We would like to thank Prof. Anand Karipot, Dr. Thara Prabhakaran for providing the NEE observations data from the CAIPEEX ground campaign at Barkachha for this study. We would like to thank Prof. Raghu Murtugudde, Dr. Tania Guha, Mr. Santanu Halder, and Mr. Vineet Singh for discussions and technical help during this study. AIRS data downloaded from (<https://disc.gsfc.nasa.gov/datasets?page=1&source=AQUA%20AIRS,AQUA%20AMSU-A,AQUA%20HSB>). Meteorological data downloaded from Era-interim Reanalysis from (<https://www.ecmwf.int/en/forecasts/datasets/reanalysis-datasets/era-interim>). Figures 1, 4, 5, and 6 were plotted using Grid Analysis and Display System (GrADS) (<http://cola.gmu.edu/grads/downloads.php>). Figures 2 and 3 were plotted using open source software R.

**Authors contributions** YKT and JVR conceptualized the study and contributed to drafting the manuscript. SG performed the analysis and written the manuscript. JVR contributed to temperature-related analysis and discussions. PKD, SC, and PG contributed with NEE observation data used in this study. PKD and SC provided inputs for CO<sub>2</sub>-related discussions in the manuscript.

**Data availability** The datasets generated during and/or analyzed during the current study are available from the corresponding author on reasonable request.

## Declarations

**Conflict of interest** Authors declare no conflict/competing interest.

## References

- Adebayo TS, Udemba EN, Ahmed Z et al (2021) Determinants of consumption-based carbon emissions in Chile: an application of non-linear ARDL. *Environ Sci Pollut Res*. <https://doi.org/10.1007/s11356-021-13830-9>



- Aubinet M, Grelle A, Ibrom A, Rannik Ü, Moncrieff J, Foken T, Kowalski AS, Martin PH, Berbigier P, Bernhofer C, Clement R, Elbers J, Granier A, Grünwald T, Morgenstern K, Pilegaard K, Rebmann C, Snijders W, Valentini R, Vesala T (1999) Estimates of the annual net carbon and water exchange of forests: the EURO-FLUX methodology. *Adv Ecol Res* 30:113–175. [https://doi.org/10.1016/S0065-2504\(08\)60018-5](https://doi.org/10.1016/S0065-2504(08)60018-5)
- Chahine M, Barnet C, Olsen ET, Chen L, Maddy E (2005) On the determination of atmospheric minor gases by the method of vanishing partial derivatives with application to CO<sub>2</sub>. *Geophys Res Lett* 32:1–5. <https://doi.org/10.1029/2005GL024165>
- Chahine MT, Chen L, Dimotakis P, Jiang X, Li Q, Olsen ET, Pagano T, Randerson J, Yung YL (2008) Satellite remote sounding of mid-tropospheric CO<sub>2</sub>. *Geophys Res Lett* 35:1–5. <https://doi.org/10.1029/2008GL035022>
- Chakraborty S, Tiwari YK, Burman PKD, Roy SB, Valsala V (2020) Observations and modeling of GHG concentrations and fluxes over India. In: Krishnan R, Sanjay J, Gnanaseelan C, Mujumdar M, Kulkarni A, Chakraborty S (eds) *Assessment of climate change over the Indian region*. Springer, Singapore. [https://doi.org/10.1007/978-981-15-4327-2\\_4](https://doi.org/10.1007/978-981-15-4327-2_4)
- Dash SK, Hunt JCR (2007) Variability of climate change in India. *Curr Sci* 93:782–788
- Dash SK, Mangain A (2011) Changes in the frequency of different categories of temperature extremes in India. *J Appl Meteorol Climatol* 50:1842–1858. <https://doi.org/10.1175/2011JAMC2687.1>
- Deb Burman PK, Shurpali NJ, Chowdhuri S et al (2020) Eddy covariance measurements of CO<sub>2</sub> exchange from agro-ecosystems located in subtropical (India) and boreal (Finland) climatic conditions. *J Earth Syst Sci* 129:43. <https://doi.org/10.1007/s12040-019-1305-4>
- Geddes JA, Murphy JG, Schurman J, Petroff A, Thomas SC (2014) Net ecosystem exchange of an uneven-aged managed forest in central Ontario, and the impact of a spring heatwave event. *Agric for Meteorol* 198–199:105–115. <https://doi.org/10.1016/j.agrfor.2014.08.008>
- Gnanamoorthy P, Selvam V, Deb Burman PK, Chakraborty S, Karipot A, Nagarajan R, Ramasubramanian R, Song Q, Zhang Y, Grace J (2020) Seasonal variations of net ecosystem (CO<sub>2</sub>) exchange in the Indian tropical mangrove forest of Pichavaram. *Estuar Coast Shelf Sci* 243:106828. <https://doi.org/10.1016/j.ecss.2020.106828>
- Golkar F, Al-Wardy M, Saffari SF, Al-Aufi K, Al-Rawas G (2020) Using OCO-2 satellite data for investigating the variability of atmospheric CO<sub>2</sub> concentration in relationship with precipitation, relative humidity, and vegetation over Oman. *Water (switzerland)*. <https://doi.org/10.3390/w12010101>
- Guha-Sapir D, Hoyois P, Below R (2016) Annual disaster statistical review 2016: the numbers and trends. CRED, Brussels. [https://reliefweb.int/sites/reliefweb.int/files/resources/adsr\\_2016.pdf](https://reliefweb.int/sites/reliefweb.int/files/resources/adsr_2016.pdf)
- IPCC 2013: Stocker TF, Qin D, Plattner GK, Tignor MMB, Allen SK, Boschung J, Nauels A, Xia Y, Bex V, Midgley PM (2013) IPCC. *Clim Chang 2013 Phys Sci Basis Work Gr I Contrib to Fifth Assess Rep Intergov Panel ClimChang* 9781107057:1–1535. <https://doi.org/10.1017/CBO9781107415324>
- Jiang X, Chahine MT, Olsen ET, Chen LL, Yung YL (2010) Interannual variability of mid-tropospheric CO<sub>2</sub> from atmospheric infrared sounder. *Geophys Res Lett* 37:1–5. <https://doi.org/10.1029/2010GL042823>
- Kim J-S, Kug J-S, Yoon J-H, Jeong S-J (2016) Increased atmospheric CO<sub>2</sub> growth rate during El Niño driven by reduced terrestrial productivity in the CMIP5 ESMs. *J Clim* 29(24):8783–8805. <https://doi.org/10.1175/JCLI-D-14-00672.1>
- Kothawale DR, Kumar KR (2005) On the recent changes in surface temperature trends over India. *Geophys Res Lett* 32:1–4. <https://doi.org/10.1029/2005GL023528>
- Kothawale DR, Revadekar JV, Kumar KR (2010) Recent trends in pre-monsoon daily temperature extremes over India. *J Earth Syst Sci* 119:51–65. <https://doi.org/10.1007/s12040-010-0008-7>
- Kumar KR, Tiwari YK, Valsala V, Murtugudde R (2014) On understanding the land-ocean CO<sub>2</sub> contrast over the Bay of Bengal: a case study during 2009 summer monsoon. *Environ Sci Pollut Res* 21:5066–5075. <https://doi.org/10.1007/s11356-013-2386-2>
- Kumar KR, Revadekar JV, Tiwari YK (2014) AIRS retrieved CO<sub>2</sub> and its association with climatic parameters over India during 2004–2011. *Sci Total Environ* 476–477(2014):79–89. <https://doi.org/10.1016/j.scitotenv.2013.12.118>
- Kumar KR, Tiwari YK, Revadekar JV, Vellore R, Guha T (2016) Impact of ENSO on variability of AIRS retrieved CO<sub>2</sub> over India. *Atmos Environ* 142:83–92. <https://doi.org/10.1016/j.atmosenv.2016.07.001>
- Lüthi D, Le Floch M, Bereiter B, Blunier T, Barnola JM, Siegenthaler U, Raynaud D, Jouzel J, Fischer H, Kawamura K, Stocker TF (2008) High-resolution carbon dioxide concentration record 650,000–800,000 years before present. *Nature* 453:379–382. <https://doi.org/10.1038/nature06949>
- MAUSAM (2016) Quarterly journal of meteorology, hydrology & geophysics, weather in India, vol 67, issue 2, pp 513–528. <https://metnet.imd.gov.in/mausamdocs/36721.pdf>
- Olsen ET, Licata SJ (2015) AIRS Version 5 Release Tropospheric CO<sub>2</sub> Products, Tech. rep., Jet Propulsion Laboratory, 38 p. [http://disc.sci.gsfc.nasa.gov/AIRS/documentation/v5\\_docs/AIRS\\_V5\\_Release\\_User\\_Docs/AIRS-V5-Tropospheric-CO2-Products.pdf](http://disc.sci.gsfc.nasa.gov/AIRS/documentation/v5_docs/AIRS_V5_Release_User_Docs/AIRS-V5-Tropospheric-CO2-Products.pdf)
- Oza M, Kishitawal CM (2015) Spatio-temporal changes in temperature over India. *Curr Sci*. <https://doi.org/10.1820/v109/i6/1154-1158>
- Pattanaik DR, Mohapatra M, Srivastava AK, Kumar A (2017) Heatwave over India during summer 2015: an assessment of real-time extended range forecast. *Meteorol Atmos Phys* 129:375–393. <https://doi.org/10.1007/s00703-016-0469-6>
- Perkins-Kirkpatrick SE, Lewis SC (2020) Increasing trends in regional heatwaves. *Nat Commun* 11(1):1–8. <https://doi.org/10.1038/s41467-020-16970-7>
- Prabha TV, Khain A, Maheshkumar RS, Pandithurai G, Kulkarni JR, Konwar M, Goswami BN (2011) Microphysics of premonsoon and monsoon clouds as seen from in situ measurements during the Cloud Aerosol Interaction And Precipitation Enhancement Experiment (CAIPEEX). *J Atmos Sci* 68:1882–1901. <https://doi.org/10.1175/2011JAS3707.1>
- Rahmstorf S, Foster G, Cahill N (2017) Global temperature evolution: recent trends and some pitfalls. *Environ Res Lett* 12:054001
- Ramarao MVS, Sanjay J, Krishnan R et al (2019) On observed aridity changes over the semiarid regions of India in a warming climate. *Theor Appl Climatol* 136:693–702. <https://doi.org/10.1007/s00704-018-2513-6>
- Rao BB, Chowdary PS, Sandeep VM, Rao VUM, Venkateswarlu B (2014) Rising minimum temperature trends over India in recent decades: implications for agricultural production. *Glob Planet Change* 117:1–8. <https://doi.org/10.1016/j.gloplacha.2014.03.001>
- Ray KCS, De US (2003) Climate change in India, as evidenced from instrumental records. *WMO Bull* 52:53–59
- Resmi EA, Murugavel P, Dinesh G, Balaji B, Leena PP, Mercy V, Sathy N, Subharthi C, Yogesh T, Anandakumar K, Prabha TV (2019) Observed diurnal and intraseasonal variations in boundary layer winds over Ganges valley. *J Atmos Solar-Terrestrial Phys*. <https://doi.org/10.1016/j.jastp.2019.03.012>
- Revadekar JV, Kumar KR, Tiwari YK, Valsala V (2016) Variability in AIRS CO<sub>2</sub> during active and break phases of Indian summer monsoon. *Sci Total Environ* 541:1200–1207. <https://doi.org/10.1016/j.scitotenv.2015.09.078>



- Rohini P, Rajeevan M, Srivastava AK (2016) On the variability and increasing trends of heatwaves over India. *Sci Rep* 6:1–9. <https://doi.org/10.1038/srep26153>
- Sanjay J et al (2020) Temperature changes in India. In: Krishnan R, Sanjay J, Gnanaseelan C, Mujumdar M, Kulkarni A, Chakraborty S (eds) *Assessment of climate change over the Indian Region*. Springer, Singapore. [https://doi.org/10.1007/978-981-15-4327-2\\_2](https://doi.org/10.1007/978-981-15-4327-2_2)
- Sathyanadh A, Prabha TV, Balaji B, Resmi EA, Karipot A (2017) Evaluation of WRF PBL parameterization schemes against direct observations during a dry event over the Ganges valley. *Atmos Res* 193:125–141. <https://doi.org/10.1016/j.atmosres.2017.02.016>
- Sen RS, Balling RC (2005) Analysis of trends in maximum and minimum temperature, diurnal temperature range, and cloud cover over India. *Geophys Res Lett* 32:1–4. <https://doi.org/10.1029/2004GL022201>
- Srivastava AK, Revadekar JV, Rajeevan M (2016) State of the climate in 2015: South Asia. *Bull Am Meteorol Soc* 97:S215–S216
- Srivastava AK, Revadekar JV, Rajeevan M (2017) State of the Climate in 2016: South Asia. *Bull Am Meteorol Soc* 98:S217–S220. <https://doi.org/10.1175/2017BAMSStateoftheClimate.1>
- Tiwari YK, Revadekar JV, Ravi Kumar K (2014) Anomalous features of mid-tropospheric CO<sub>2</sub> during Indian summer monsoon drought years. *Atmos Environ* 99:94–103. <https://doi.org/10.1016/j.atmosenv.2014.09.060>
- Udemba EN (2020) Mediation of foreign direct investment and agriculture towards ecological footprint: a shift from single perspective to a more inclusive perspective for India. *Environ Sci Pollut Res*. <https://doi.org/10.1007/s11356-020-09024-4>
- Udemba EN, Güngör H, VictorBekun F, Kirikkaleli Güngör H, VictorBekun F, Kirikkaleli D (2021) Economic performance of India amidst high CO<sub>2</sub> emissions. *Sustain Prod Consum* 27:52–60. <https://doi.org/10.1016/j.spc.2020.10.024>
- Valsala V, Tiwari YK, Pillai P, Roxy M, Maksyutov S, Murtugudde R (2013) Intraseasonal variability of terrestrial biospheric CO<sub>2</sub> fluxes over India during summer monsoons. *J Geophys Res Biogeosci* 118:752–769. <https://doi.org/10.1002/jgrg.20037>
- Wohlfahrt G, Gerdel K, Migliavacca M, Rotenberg E, Tatarinov F, Müller J, Hammerle A, Julitta T, Spielmann FM, Yakir D (2018) Sun-induced fluorescence and gross primary productivity during a heatwave. *Sci Rep* 8:1–9. <https://doi.org/10.1038/s41598-018-32602-z>
- Wu L, Hasekamp O, Hu H, Landgraf J, Butz A, Aan De Brugh J, Aben I, Pollard DF, Griffith DWT, DiG F, Koshelev D, Hase F, Toon GC, Ohyama H, Morino I, Notholt J, Shiomi K, Iraci L, Schneider M, De Mazière M, Sussmann R, Kivi R, Warneke T, Goo TY, Té Y (2018) Carbon dioxide retrieval from OCO-2 satellite observations using the RemoTeC algorithm and validation with TCCON measurements. *Atmos Meas Tech* 11:3111–3130. <https://doi.org/10.5194/amt-11-3111-2018>

**Publisher's Note** Springer Nature remains neutral with regard to jurisdictional claims in published maps and institutional affiliations.